Simulating diluted bitumen spills in boreal lake limnocorrals- Part 2: Factors affecting the physical characteristics and submergence of diluted bitumen

Stoyanovich, S[a]., Rodríguez-Gil, JR[b]., Hanson, M[c]., Hollebone, B.P[d]., Orihel, D. M[e]., Palace, V[b]., Faragher, R[d]., Mirnaghi, F.S[d]., Shah, K[d]., Yang, Z[d]., Blais, J.M[a*]

[a] Department of Biology, University of Ottawa, Ottawa, Ontario, K1N 6N5, Canada

[b] International Institute for Sustainable Development - Experimental Lakes Area, 111 Lombard Avenue, Suite 325, Winnipeg, Manitoba R3N 0T4, Canada

[c] Department of Environment and Geography, University of Manitoba, Winnipeg, MB, R3T 2N2, Canada.

[d] Emergencies Science and Technology Section, Environment and Climate Change Canada, Ottawa, Ontario, Canada

[e] Department of Biology and School of Environmental Studies, Queen's University, Kingston, ON K7L 3N6

Corresponding author: Jules Blais
Department of Biology
University of Ottawa
20 Marie-Curie
Ottawa, ON, Canada K1N 6N5,
Tel: +1 (613) 562-5800 ext. 6650
Email: jules.blais@uottawa.ca

Abstract

We examined the fate and behaviour of diluted bitumen (dilbit) as it weathered for 70 days in freshwater limnocorrals (10 m diameter x 1.5 m depth) installed in a boreal lake to simulate dilbit spills in a natural aquatic environment. We added seven different dilbit spill volumes, ranging from 1.5 to 180 L, resulting in oil-to-water ratios between 1:71 000 (v/v, %) and 1:500 (v/v, %). Volatile hydrocarbons in the dilbit slick decreased rapidly after the dilbit was spilled on the water's surface, and dilbit density and viscosity significantly increased (> 1 g mL^{-1} and > 5 000 000 mPa s, respectively). Dilbit sank to the bottom sediments in all treatments, and the time to sinking was positively correlated with spill volume. The lowest dilbit treatment began to sink on day 12, whereas the highest dilbit treatment sank on day 31. Dilbit submerged when its density surpassed the density of freshwater (> 0.999 g mL^{-1}), with wind, rain, and other factors contributing to dilbit sinking by promoting the break-up of the surface slick. This experiment improves our ability to predict dilbit's aquatic fate and behaviour, and its tendency to sink in a boreal lake. Our findings should be considered in future pipeline risk assessments to ensure the protection of these important aquatic systems.

Keywords

Dilbit; Natural weathering; Limnocorral; Submerged oil; Freshwater

1.0 Introduction

Landlocked deposits of bitumen are found in many places worldwide, including Venezuela, the United States, and Russia, but the largest deposits are found in Alberta, Canada. Following extraction, crude bitumen is too dense and viscous to flow and must be engineered to meet pipeline specifications. Diluents, consisting of light hydrocarbon condensates, are mixed with bitumen to reduce its density and viscosity to pipeline specifications (0.940 g mL^{-1} and 350 mPa·S, respectively), generating a blend of crude oil known as diluted bitumen, or dilbit (Fingas, 2015a). Pipelines, despite being one of the safest modes of transporting Canada's dilbit to market (Green and Jackson, 2015; Transport Canada, 2013), are still vulnerable to oil spills. From 2010 to 2018, a total 1.3 billion m^3 of crude oil was transported out of Canada, by pipeline and railway combined (CER, 2019), of which an estimated 14 000 m^3 was spilled in Canada (Oliver Wyman, 2019). Such spills are likely to continue, in part because some estimates forecast a million barrels per day (b/d) increase in oil sands production in the next decade (CAPP, 2019; CER, 2016).

Several recent reports identified knowledge gaps in the fate and behaviour of spilled dilbit in freshwater (Lee et al., 2015; NASEM, 2016; 2014, 2013; Transportation Research Board and National Research Council, 2014). Following a spill to water, dilbit's physical and chemical characteristics change due to evaporation, emulsion, and other processes. Evaporation results in significant loss of oil mass as lighter hydrocarbons are lost to the atmosphere. Evaporation increases both the viscosity and density of the oil, and contributes to eventual oil submergence (Stoyanovich et al. 2019; King et al., 2017, 2014; Lee et al., 2015; NASEM, 2016). These weathering processes

affect oil spill remediation strategies that must consider the physical properties of the spilled oil. For example, *in-situ* burning can remove oil from the water surface but it is only efficient when the volatile components are still present and the slick is >2 mm thick (Fingas, 2015a). For any heavy oil, including dilbit, the window of opportunity to ignite the oil is within the first 1 to 2 hours of the spill (Federici and Mintz, 2014). Chemical dispersants can diffuse the oil into the water column (Canevari, 1978), but dispersants don't work when oil viscosity exceeds 5 000 to 10 000 mPa·s (Federici and Mintz, 2014; ITOPF, 2011; Nordvik, 1995; Zhao et al., 2014). Mechanical skimmers and booms are ineffective when oil viscosity is > 100 000 mPa·s (Federici and Mintz, 2014; ITOPF, 2012; Wadsworth, 1995).

Uncertainty remains about the environmental fate of dilbit, including its tendency to sink or float in freshwater (Lee et al., 2015). For example, studies documented dilbit submergence after a pipeline ruptured in Marshall, Michigan in 2010. The rupture released 3.2 million litres of dilbit into Talmadge Creek and eventually the Kalamazoo River, where 10-20% of the spilled oil sank upon entering the river (Fitzpatrick et al., 2015; Lee et al., 2015; US EPA, 2013). The spill occurred during high rainfall and flooding that increased the turbulence and suspended sediments in the river flows (Fitzpatrick et al., 2015). Interaction between suspended sediment and floating oil forms macroscopic sediment-oil aggregates (SOAs, > 1 mm) and microscopic oil-particulate aggregates (OPAs, < 1 mm) that may become dense enough to sink (Gustitus and Clement, 2017), which was likely the case in the Kalamazoo River spill (Fitzpatrick et al., 2015). Only 6 – 10 % of the submerged oil was recoverable by dredging three years

following the spill (US EPA, 2013), an estimated ~ 300 000 L of submerged dilbit remained at the bottom of the Kalamazoo River (NASEM, 2016).

Experimental studies under controlled environments have also documented dilbit weathering and sinking. Hua et al. (2018) mixed artificially weathered Cold Lake Blend (CLB) dilbit with saltwater containing 10 000 mg L^{-1} suspended sediments in test tubes and found that the resulting OPAs sank. Waterman and Garcia (2015) mixed artificially weathered dilbit with river sediments to form small oil droplets coated in sediments that experienced both neutral buoyancy and submergence in tap water. Laboratory studies, however, may not capture important environmental factors like solar radiation, microbial interactions, or diurnal and seasonal changes (Lee et al., 2015). Short (2013) noted that laboratory studies consider low wind speeds and high slick thicknesses that may be unrealistic of an actual spill scenario. Field experiments are therefore needed to assess dilbit weathering over longer timespans and under natural environmental conditions (Lee et al., 2015).

Several studies have investigated the fate of dilbit in outdoor field experiments to address some of the limitations of laboratory experiments. King et al. (2014) simulated dilbit spills in a flume tank containing filtered seawater and allowed the oil to weather for 13 days, noting increases in dilbit's density and the presence of small submerged oil droplets. Stoyanovich et al. (2019) added dilbit into outdoor tanks containing natural lake water and sediments. The researchers found that dilbit sank after 8 days when evaporation and emulsification caused dilbit density to surpass freshwater density. Despite these developments, questions remain about whether dilbit will float, disperse, or sink, especially in freshwater systems (Lee et al., 2015).

Here, we investigated the fate of dilbit in a large-scale spill experiment to assess dilbit's propensity to weather and submerge in a natural lake environment. This study was part of the BOREAL project (Boreal Lake Oil Release Experiments by Additions to Limnocorrals), a multi-phase program to examine the fate, behavior, and impacts of dilbit spills in freshwater environments. This study expands on a pilot study involving dilbit additions into three outdoor 2-meter diameter tanks (Cederwall et al., 2020; Stoyanovich et al., 2019). We installed nine 10-m diameter limnocorrals in a boreal lake near Kenora, Ontario, Canada to simulate a pipeline spill to freshwater. To these limnocorrals we added dilbit in volumes ranging from 1.5 L to 180 L, employing a regression design to simulate dilbit spills ranging in actual oil:volume ratios between 1:71 000 and 1:500 (Rodriguez-Gil et al., In Prep). This study reports the physical and chemical changes associated with dilbit spills exposed to natural biotic and abiotic environmental conditions typical of a boreal lake for 70 days. We examined each limnocorral treatment individually and utilized our regression design to determine how spill volume correlated to different outcomes, namely, sinking times and weathering rates. This study provides a novel approach to determine environmentally relevant timelines for major dilbit weathering processes in a natural freshwater system to inform risk assessors, spill responders, and regulators involved in oil spill countermeasures.

2.0 Methodology

2.1 Study Site

We performed this study in Lake 260 at the International Institute for Sustainable Development - Experimental Lakes Area (IISD-ELA) near Kenora, Ontario, Canada

during the summer of 2018. The IISD-ELA is a remote freshwater research site located on the Precambrian Shield of northwestern Ontario (49°40'N, 93°44'W). IISD-ELA consists of 58 boreal lakes of various dimensions. In 1968, the federal government of Canada and the province of Ontario designated this site for experimental freshwater studies (Johnson and Vallentyne, 1971). Lake 260 is a clear, oligotrophic lake 32.8 ha in area with a maximum depth of 15.7 m and an approximate water volume of 1 975 000 m^3.

2.2 Experimental Design

We installed nine limnocorrals in a ~ 2-m deep littoral zone on the northern shore of Lake 260 at the IISD-ELA. Rodríguez-Gil et al. (In Prep) provided details about the limnocorrals, their construction, and other elements of the larger study design. Briefly, we installed limnocorrals that consisted of a 10 m diameter floating ring to which we attached a high-density polyethylene (HDPE) cylindrical membrane extending down to the sediments. We used sandbags to seal the plastic membrane to the lake bottom (Figure 1A), a typical procedure in limnocorral studies (Baulch et al., 2003; Orihel et al., 2006). We accounted for potential water leakage throughout the experiment by tracking tritium (^3H) that we initially spiked to all limnocorrals.

We randomly assigned seven of the nine limnocorrals a nominal dilbit spill volume of either 1.5, 2.9, 5.5, 18, 42, 82, or 180 L in the form of a regression design. The rationale for the spill volume selection is presented in the companion publication by Rodríguez-Gil et al. (In Prep). The remaining two limnocorrals were controls; one located adjacent to dilbit treatments (near field) and one located roughly 100m from any

dilbit treatments (far field) (Figure 1B and C). We added Cold Lake Winter Blend (CLWB) dilbit to the water's surface of these limnocorrals on June 20th 2018, between 8:30am and 10:00am. We pumped CLWB from cans to the water surface using a Flojet diaphragm pump (FLOJET Corp, California) at a rate of approximately 7.5 L min^{-1} (Figure S1). We weighed all empty cans, hoses, and pumps before and after the dilbit additions to precisely determine the mass of dilbit added to each limnocorral. We then estimated spill volumes from the mass of CLWB added and its density measured at 15 ºC (0.9215 g mL^{-1}). Shah et al. (2019) provides additional details of the procedure for pumping dilbit to water. We monitored these limnocorrals for 70 days, tracking changes in dilbit properties until we decommissioned the experiment on September 8th, 2018, and remediated the site (Rodriguez-Gil et al., In Prep).

2.3 Environmental and Water Quality Monitoring

We installed a portable meteorological station on a small island adjacent to the study site at lake-level on June 15th 2019, 5 days before the dilbit addition. The meteorological station recorded wind speed and direction, precipitation, air temperature, humidity, and solar radiation every hour for the study's duration. We installed HOBO® data loggers at 0.5 m below water surface in each of the limnocorrals that recorded light intensity and water temperature every 4 minutes for the duration of the study. We sampled water for a full suite of water quality parameters (e.g. turbidity, ions, and nutrients) in each of the nine limnocorrals throughout the experiment. These details are in a companion paper (Rodriguez-Gil et al., In Prep).

187 *2.4 Dilbit Slick Behavioural Monitoring*

188 We monitored the dilbit slicks daily, taking note of any changes in colour,
189 thickness, surface area coverage, and sinking patterns. Underwater cameras (GoPro
190 Hero 5 Session®) enabled the qualitative assessment of dilbit dispersal and presence
191 on the sediment bottom. We recorded the surface behaviour of the low, medium, and
192 high treatment (1.5, 18, and 180 L) from sunrise to sunset using time-lapse cameras
193 (Brinno TLC200 Pro HDR®) mounted 3m above the limnocorrals. Additionally, we
194 recorded aerial drone photos and videos regularly at a height of 10 m above the
195 limnocorrals to further assess slick behaviour (DJI Mavic Air Quadcopter®). We
196 processed aerial photos using ImageJ software version 1.50 to estimate temporal
197 changes in the surface area coverage of the dilbit slicks and sheens at each time a
198 photo was taken.

199

200 *2.5 Dilbit Slick Samples*

201 We collected two sets of dilbit surface slick samples from each of the limnocorral
202 treatments, one for physical measurements and one for chemical analysis, after 0.25, 2,
203 4, 8, 15, 22, 28, 42, 56, and 70 d post-spill (Figure 1D). The dilbit slicks eventually
204 submerged, which affected the dilbit sampling, and therefore the final slick sampling
205 days ranged from 15 d to 70 d depending on when submergence in each treatment
206 occurred (discussed in section 3.1).

207 We additionally collected higher volume dilbit samples (~50 mL) from the two
208 highest dilbit treatments (82 and 180 L) for physical property analysis. An Anton Paar
209 DMA 5000 and DMA 48 density meter enabled the measurement of oil density at 0, 15,

and 30 °C following ASTM D5002 (ASTM D5002-19, 2019). We measured dynamic viscosity at three different temperatures (0, 15, and 30 °C) using Anton Parr Stabinger SVM 3000 Viscometer following standard D7042 (ASTM D7042-16, 2016) and a HAAK VTiQ Viscotester (Thermo Fischer Scientific). We evaluated the Newtonian and Non-Newtonian behavior of the oil, and measured viscosity at different shear rates in any samples exhibiting non-Newtonian behavior (i.e. viscosity dependent on shear rate). Karl Fischer titration with a Metrohm 901 automatic titrator following ASTM E203 (ASTM E203-16, 2016) enabled water content determinations of each dilbit sample. We ran all dilbit samples collected for physical properties in triplicate to assess analytical accuracy.

We sampled the dilbit slick by passing a small piece of Teflon sheet along the dilbit slick until roughly 2 – 5 mL of dilbit had adhered to the material. An Agilent 7890A gas chromatograph equipped with a flame ionization detector (GC-FID) enabled analysis of total petroleum hydrocarbons, which we then grouped into four chemical fractions; F1 (< nC$_{10}$), F2 (nC$_{10}$ - nC$_{16}$), F3 (nC$_{16}$ – nC$_{34}$), and F4 (> nC$_{34}$). We used an Agilent 7890A gas chromatograph equipped with an Agilent 5975C mass selective detector (GC-MSD) to analyze petroleum biomarker compounds including: terpanes, hopanes, and steranes following the procedure in Yang et al. (2017). See section 2.0 of supporting info for more information on analytical procedures.

2.6 Chemical weathering

We normalized TPH concentrations to 17α(H) 21β(H) hopane (C$_{30}$ hopane), a recalcitrant compound termed “biomarker” to act as a recalcitrant tracer to assess weathering (Prince et al., 1994; Stout and Wang, 2016; Venosa et al., 1997). The

233 percentage of chemical remaining can be calculated by Eq. (1) adapted from Douglas et
234 al. (1996) and Radović et al (2014):
235 % analyte depleted = [1 – (C_t/C_o)(H_o/H_t) x 100] (1)
236 where C_t and C_o are the concentrations of a compound in a weathered (*t)* and original
237 (o) sample, respectively and H_t and H_o are the concentrations of C_{30} Hopane in those
238 same samples.
239
240 *2.7 Physical property models*
241 We carried out a temporal analysis of physical properties (density and viscosity)
242 on the two highest dilbit treatments (82 and 180 L) due to sample volume requirements.
243 We fit the experimental data to a hyperbolic model adapted from King et al. (2019,
244 2017, 2014):
245 $$\rho = \rho_0 + (\rho_f - \rho_0)\left(\frac{t}{T+t}\right)^n \quad (2)$$
246 $$\nu = \nu_0 + (\nu_f - \nu_0)\left(\frac{t}{T+t}\right)^n \quad (3)$$
247 Equations 2 and 3 predict temporal changes in density (ρ) and viscosity (ν) from initial
248 (ρ_0 and ν_0) to final (ρ_f and ν_f). Where "*t"* represents time (d), *"T"* is a time constant
249 representing the time (d) it takes for the density and/or viscosity to increase half-way
250 between initial and final values, and the power *"n"* controls the rate of increase.
251
252 **3.0 Results & Discussion**
253 *3.1 Physical Behaviour*
254 The slicks began to spread across the surface area of the limnocorrals
255 immediately following the dilbit. The average wind speed and air temperature was 1.4 m

256 s^{-1} and 22.4 °C, respectively on the day of dilbit addition (Rodriguez-Gil et al., In Prep).
257 The experiment was in a sheltered boreal lake and therefore did not experience any
258 breaking waves over the study duration. We noted that the distribution and thickness of
259 the dilbit slicks were largely dependent on wind speed and direction throughout the
260 experiment. Days of high wind forced the slicks to accumulate along the leeward side of
261 the limnocorral walls, increasing slick thickness, and days of low wind allowed the slicks
262 to spread, decreasing the thickness (Figure 2).

263 The dilbit slicks changed considerably in overall appearance (i.e., colour,
264 thickness, and surface skin) during the 70-d experiment (Figure S2, S3, S4, & S5).
265 Colour changes from dark black to light brown began as early as day 6 (June 26) and
266 were caused by the uptake of water droplets (Lee et al., 2015) and exposure to sunlight
267 (Bobra and Tennyson, 1989). We also observed the formation of a skin on the surface
268 of the dilbit slicks, a similar finding to a previous study by Stoyanovich et al. (2019).
269 Surface skins tend to persist in low energy systems that lack substantial turbulence or
270 agitation energy, such as Lake 260. The skins are caused by the accumulation of polar
271 compounds, including asphaltenes and resins, at the oil – water interface (Fingas,
272 2015a; Hollebone et al., 2011; Lee et al., 2015).

273 The slicks broke apart into discrete masses as weathering proceeded. We
274 observed the presence of tar balls (<10 cm in diameter), tar patties (>10 cm in
275 diameter), and tar mats (≥1 m) (Lee et al., 2015; Warnock et al., 2015) that encompass
276 a highly weathered exterior crust and a less-weathered interior (Figure S3A). A
277 precipitation event (14.3 mm in 3 h) and high winds (maximum of 6.6 m s^{-1}) on day 14
278 contributed to the break-up of the surface slicks. The tar balls remained intact for the

279 remainder of the study, becoming neutrally buoyant in the water column, and eventually
280 began to submerge to the bottom sediments (Figure S3).

281 Notably, the surface slicks in all seven treatments sank to the sediments during
282 the study period as small discrete tar balls and patties (Figure S6 & S7) and in some
283 cases large tar mats (Figure S8). The onset and completion of sinking differed among
284 treatments. Sinking onset (i.e., time when dilbit was first observed on sediments) and
285 completion (i.e., no remaining surface oil) proceeded in the following order for each
286 treatment: Day 12 – 19 (1.5 L), 14 – 22 (2.9 L), 15 – 25 (5.5 L), 14 – 28 (18 L), 15 – 43
287 (42 L), 22 – 61 (82 L), and 31 – 77 d (180 L), respectively (Figure 3A, Figure S9). We
288 found a significant positive correlation between the amount of dilbit added and the time
289 to sinking onset (*slope*=0.10, R^2 = 0.92, p<0.0005, Figure 3B), and the time to complete
290 submergence (*slope*=0.33, R^2 = 0.97, p<0.0005, Figure 3B). Note that sinking times
291 were based on the first visual appearance of dilbit on the sediment bottom, and do not
292 consider dilbit droplets dispersed or neutrally buoyant in the water column. We
293 performed visual underwater scans of the sediments every morning upon arrival at the
294 site, so any observed submergence could have occurred the previous evening, night or
295 early morning. Therefore, we may have slightly overestimated our sinking times by
296 several hours.

297 According to Hansen et al. (2015), the four major criteria that influence crude oil
298 submergence are oil density, water turbidity, water salinity, and suspended sediment
299 load. These researchers suggested dilbit submergence will most likely occur in shallow
300 streams or rivers with high suspended sediment load. When oil mixes with sediments,
301 the newly formed sediment-oil aggregates, SOAs (Gustitus and Clement, 2017), can

become denser than the water and sink. This situation may be expected when oil strands on shore and mixes with sediments suspended by wave action (Michel et al., 2014). Johannessen et al. (2019) remarked that most lab studies demonstrated dilbit sinking when dilbit was mixed with suspended sediment concentrations ranging from 1000 to 10 000 mg L^{-1}, loadings similar to maximum concentrations found in coastal river outflows (Hua et al., 2018). These total suspended sediment (TSS) loads are three to four times greater than the greatest TSS value, 2.0 mg L^{-1}, observed in any of the limnocorrals throughout our study (Figure S10). Furthermore, turbulent mixing is required to promote the interaction of the oil with the sediments (Yang et al., 2018). The low TSS concentrations along with the low mixing energy of our limnocorral systems suggests that the formation of SOAs did not play a major role in the observed submergence patterns, similar to results found in previous tank-based studies by Stoyanovich et al. (2019) and King et al. (2014).

Precipitation may have also influenced dilbit sinking. We noted that slick weathering rates were not equal among treatments, as shown by their differences in colour and buoyancy. Furthermore, small sections of the bulk floating slicks would sink below the water level while remaining attached to the floating portion (Figure S11). A number of early precipitation events (25 mm on day 7 and 8mm on day 9) occurred prior to any observed submergence (Figure S10). On days of heavy precipitation, rain was sufficient to break the slicks apart, thus separating the discrete floating and sinking sections, in a similar manner to a previous study (Stoyanovich et al., 2019).

3.2 Temporal changes in physical and chemical properties

3.2.1 Volatile Loss

The most volatile components of dilbit were the first to evaporate from the residual floating slicks (Figure 5A). We used the depletion of $\leq C_{16}$ hydrocarbons, obtained by summing concentrations of F1 and F2 fractions generated by GC-FID, to assess early evaporation of volatile components. For example, Gros et al. (2014) found that 50% of hydrocarbons $\leq C_{16}$ disappeared from oil sheens after 1 h of an experimental spill of Norwegian Grane crude oil in the open sea.

In all treatments, > 80% of the initial amount of $\leq C_{16}$ hydrocarbons was lost by the final sampling day (Figure 4A). The volatile hydrocarbon fraction nearly disappeared entirely from the slicks by the end of the study, consistent with the predictions of Gros et al. (2014)'s transport model. Conversely, the higher molecular weight F3 ($C_{16} – C_{34}$) and F4 ($> C_{34}$) fractions varied throughout the study (Figure S12) but never exceeded losses greater than 47 % across all treatments. These compounds would not likely evaporate and would be less susceptible to other forms of degradation, explaining their relative stability. Overall, the majority of volatile loss occurred within the first four days of the study, during which the average air temperature and wind speed was 21 ºC and 1.7 ms^{-1}, respectively. This rapid loss of volatile constituents is likely attributable to evaporation, an important weathering process that is responsible for early mass loss in oil residues (Gros et al., 2014; Harrison et al., 1975). Evaporation affects all crude oil types differently and will largely depend on air temperature (Fingas, 2004) and film thickness (Fingas, 2015b; Yarranton et al., 2015). Dilbit is unique because it is a heavy oil that still retains a high proportion of lower molecular weight compounds in its diluent, and thus it

evaporates more than other conventional heavy oils (Government of Canada, 2014; Hansen et al., 2015). Yarranton et al. (2015) found that CLWB evaporation accelerated at higher temperature and lower film thickness, but was unaffected by wind speed. The researchers suggested that dilbit evaporation was limited by the mass transfer of volatiles in bitumen, which is limited by it's high viscosity.

The thickness of the dilbit layer can affect the diffusion of volatiles at the oil – air interface, resulting in less evaporation from thick slicks compared to thin sheens (Lee et al., 2015). For example, King et al (2017) found that increasing the thickness of dilbit slicks from 4 to 7 mm reduced the weathering of the oil in tank based studies. In our study, we were unable to track slick thickness, however we used spill volume as a proxy for slick thickness because the surface area of the limnocorrals was fixed. The regression design allows us to analyze the relationship between volatile loss and dilbit-spill volume at each of the sampling timepoints using simple linear regressions (Figure 4B). A significant slope estimate (i.e. $p < 0.05$) indicates a relationship between the volatiles remaining in the dilbit slick and the amount of dilbit spilled. We observed significant positive slope estimates at only two time points (1 and 8 d) throughout the study, individual regressions can be found in Figure S13. In general, slopes were greater than 0 for the majority of sampling time points, indicating that the volatiles remained in the higher volume slicks for longer periods of time. The thin sheens found in lower dilbit treatments evaporated faster than the sheens from the thicker oil slicks in the higher treatments. These findings corroborated both laboratory and mesoscale field studies where mass transfer of volatile compounds through the dilbit film decreased with increasing film thickness (Brandvik and Faksness, 2009; Yarranton et al., 2015). Other

371 factors affecting evaporation rates are climatic parameters such as temperature
372 (Fingas, 2004; King et al., 2019). Yarranton et al (2015) have shown that the
373 evaporation rate of CLWB increases with increasing temperature consistent with
374 decreasing viscosity and more rapid diffusion of the volatiles out of the slick. We
375 conducted our study during the warm summer months on a relatively small, sheltered
376 lake (i.e., high air temperature and limited spreading), therefore we would likely observe
377 higher evaporation rates in a larger open system (i.e., more spreading) and lower
378 evaporation rates at lower temperatures.

379 The dilbit slicks remained heterogeneous throughout the entire study, therefore
380 sample variability was high. The dilbit samples in the lowest volume treatments would
381 consist of a sheen on low wind days (i.e. more spread out) and thick oil slick on high
382 wind days (i.e. when dilbit accumulated at one side of the limnocorral), which may
383 explain some of the variability in the results. Without controlling and differentiating
384 between surface and bulk dilbit slick samples, processes such as photooxidation, which
385 would be most prominent on the outermost film of the dilbit slick, are difficult to discern
386 in this study. Biodegradation may have played a role in the removal of the lower
387 molecular weight hydrocarbons because these simple compounds are most susceptible
388 to microbial decomposition (Prince et al., 2003). However, microbes are unlikely to
389 affect the rapid and early losses of low molecular weight hydrocarbons in this study.
390 Biodegradation tends to occur over long timeframes (Lee et al., 2015) and in systems
391 that are naturally exposed to petroleum hydrocarbons, such as natural oil seeps, which
392 facilitate the proliferation of hydrocarbon degrading bacteria (Atlas and Hazen, 2011).
393 Future work is thus planned to analyze compositional changes in the weathered dilbit

394 samples in order to differentiate between other roles of degradation, including
395 biodegradation and photooxidation.
396
397 *3.2.2 Density and Viscosity*
398 The rheological changes that occur to oil following a spill are important to
399 consider as they can influence the spill response options that follow. We fit dilbit density
400 data obtained from the surface slicks of our two highest treatments (180 and 82 L) to
401 equation (2) and obtained the following:
402 180 L; $\rho = 0.9215 + (1.0024 - 0.9215)\left(\frac{t}{6.35+t}\right)^{0.148}$
403 82 L; $\rho = 0.9215 + (1.0112 - 0.9215)\left(\frac{t}{49.7+t}\right)^{0.128}$
404 Dilbit density (measured at 15 °C) increased rapidly within the first 8 days and
405 then at a more gradual rate for the remainder of the study (Figure 5A). After just 24
406 hours of environmental exposure, density values in both the 82 and 180 L treatments
407 were 0.9854 and 0.9785 g mL^{-1}, respectively. These reported 24 hour values were
408 slightly greater than values reported from wave tank studies by King et al. (2014), where
409 CLB reached a density of 0.96 g mL^{-1} after 24 h, and similar our previous tank based
410 study where the density of CLB reached 0.9883 g mL^{-1} after 24 h (Stoyanovich et al.,
411 2019). Maximum densities occurred on day 28 in the 82 L treatment (1.0057 g mL^{-1})
412 and day 56 in the 180 L treatment (1.0072 g mL^{-1}) and were substantially higher than
413 the density of the fresh dilbit (Table S1). Sunken tar balls collected from the sediment
414 bottom of the 180, 82, 42, and 18 L treatments had densities of 0.9999, 1.0016, 1.0042,
415 and 1.0094 g mL^{-1}, respectively. These values are equal to or higher than the density
416 range of freshwater that would be expected throughout the experiment considering a

maximum water density of 0.9999 g mL^{-1} is reached at 4 ºC (Weast et al., 1988). Dilbit density can increase from the loss of volatiles. We noted that the density of the weathered dilbit was linearly correlated with the amount of volatile hydrocarbon loss in both 180 and 82 L treatments (Slope = 0.00071, R^2= 0.79, p <0.005, Figure S15A). Dilbit returns to a physical state similar to dense and viscous bitumen as the diluent evaporates away (Government of Canada, 2014; Yarranton et al., 2015). Water uptake through emulsification may have also affected the density increases, where water content increased to approximately 20% in the residual dilbit and then stabilized after 15 d, roughly the same time that density measurements stabilized (Figure 5A, Figure S15).

We fit the $\log_{10}$ transformed viscosity data to equation (3) and yielded:

180 L, $\upsilon = 188 + (1.0 \times 10^{12} - 188)\left(\frac{t}{9717+t}\right)^{2.25}$

82 L, $\upsilon = 184 + (4.0 \times 10^{7} - 184)\left(\frac{t}{104+t}\right)^{1.79}$

Viscosity (measured at 15 °C) increased rapidly after the onset of the spills, exceeding 100 000 mPa·s after just 4 and 8 d in the 82 and 180 L treatments, respectively, resulting in a > 500-fold change from the initial viscosity (Figure 5B). Throughout the remainder of the study, viscosity measurements continued to increase, eventually reaching > 5 000 000 (27 000-fold change) and 30 000 000 mPa·s (170 000-fold change) in the 82 and 180 L treatments, respectively at the end of the study. The temporal change in viscosity was similar to density in that the 82 L treatment reached greater values early on, and then was surpassed by the 180 L treatment between day 42 and 56. These high viscosity values would limit the potential for dispersion into the water column in the form of small droplets, thus further reducing the potential to interact with suspended sediments.

Viscosity changes can be attributable to multiple processes. First, evaporation alone can return the viscosity to a value similar to crude bitumen (i.e., 100 000 – 450 000 mPa·S) (Fingas, 2015a), similarly to density, viscosity was linearly correlated with the amount of volatile hydrocarbon loss in both 180 and 82 L treatments (Slope = 0.047, R^2= 0.79, p <0.005, Figure S15B). Second, the dispersion of small water droplets into the dilbit slick can further increase viscosity due to internal friction between water droplets and the dilbit structure (Brandvik and Faksness, 2009; Fingas, 2015a; Fingas and Fieldhouse, 2004). The water content of collected dilbit samples increased early in the study and then plateaued at values between 18 – 25% after 8 d, remaining stable for the remainder of the study (Figure S14). The interaction of water droplets with dilbit under various environmental conditions can lead to the formation of water-in-oil emulsions of which there exists four main types; 1) stable, 2) meso-stable, 3) entrained, and 4) unstable. These are classified according to the visual appearance, water content, stability and rheological properties of the oil which are often dependent on the oil's chemical composition and environmental factors such as temperature, mixing energy of the system (Fingas and Fieldhouse, 2014a), and salinity of water (Lee et al., 2015). Based on the properties of each emulsion outlined by Fingas and Fieldhouse (2014b), the slicks measured in this study fit into the entrained category. This classification is similar to our earlier pilot study, where the water content of dilbit samples remained <20%, becoming too dense and viscous for any additional water droplet penetration (Stoyanovich et al., 2019).

Wave energy can often facilitate the formation of emulsions by forcing small water droplets into the oil matrix, but if the oil is too viscous the droplets will not

efficiently enter the oil slick (Fingas, 2015a). Rainfall could provide some turbulence to promote water uptake, however the first major rainfall event post-spill (25 mm) did not occur until day 7 (Figure S10). In our study, the dilbit viscosity exhibited greater than 5 000-fold increase by day 8, the same time at which the water content stabilized, suggesting that the dilbit was too viscous to further incorporate any water droplets (Fingas, 2015a). Therefore, it is likely that the high viscosity of the dilbit paired with the relatively low energy of our study lake limited the formation of any stable form of emulsion, which would require water content to be between 70-80% (Fingas and Fieldhouse, 2014a).

The substantial increases in viscosity observed in this study could limit the feasibility of many response options following the spill. Viscosities exceeded the threshold for chemical dispersant use (i.e., >5 000 mPa·S) after just 6 h of environmental exposure (Federici and Mintz, 2014; ITOPF, 2011; Nordvik, 1995; Zhao et al., 2014). Viscosities surpassed the limit for efficient mechanical recovery techniques (i.e., 100 000 mPa·S), including booms and skimmers, after just 4 d (Federici and Mintz, 2014; ITOPF, 2012; Wadsworth, 1995). Our results suggest that following a summer dilbit spill in a boreal lake, spill responders would need to employ recovery techniques within the first 6 hours to 4 days of the spill in order to achieve efficient recovery. Response times are largely dependent on the remoteness of the spill site. The Canadian response organization standards require on-water recovery operations to be completed within 10 operational days after the recovery equipment is first deployed on site (Transport Canada, 1995). While deployment times for accessible coastal areas can range from 6 hours to 3 days (Transport Canada, 1995), the logistical challenges of

a spill in a remote location could extend response timelines and result in a significant amount of dilbit that has sunken to the sediments.

4.0 Conclusion

Reports have suggested the potential for dilbit to sink in fresh and marine water under high energy conditions with high suspended sediment loads and after sufficient weathering (Fitzpatrick et al., 2015; Government of Canada, 2014; Hansen et al., 2015; Hua et al., 2018). Here we showed that dilbit is capable of sinking under natural conditions of an oligotrophic freshwater lake with very low suspended sediment loads and mixing energy, suggesting that dilbit will sink due to weathering alone and was not likely attributable to the interaction with suspended particles. The evaporative loss of volatiles coincided with increases in density and viscosity, returning dilbit to a condition similar to that of crude bitumen. Dilbit's viscosity quickly surpassed important threshold values for different spill response methods. Therefore, under these environmental conditions, the use of traditional response techniques including *in-situ* burning, chemical dispersants, booms, and skimmers would become highly inefficient within the early days of the spill.

This study highlights the rapid physical and chemical changes that follow dilbit spills under realistic conditions typical of a boreal lake. The realistic nature of this work provides novel information on dilbit's fate in freshwater, building from laboratory and tank studies, and focusing on realistic conditions typical of a boreal lake. Simulating a wide variety of spill sizes over long periods of time (i.e. 70 days) has allowed us to determine for the first time the influence that spill volume can have on important

509 physical processes including sinking. The outcome of this study will provide decision
510 makers with critical new information to consider when planning dilbit transport in the
511 future.
512
513 **Acknowledgements**
514 Funding for the present study was provided by a Natural Sciences and
515 Engineering Research Council Strategic Partnership Grant (STPGP 493786-16
516 awarded to J.M. Blais, M. Hanson, and D.M. Orihel), a grant under the Oceans
517 Protection Program, in-kind contributions from Environment and Climate Change
518 Canada (ECCC), and in-kind support from the IISD-Experimental Lakes Area. A special
519 thank you to J. Séguin, T. Black, J. Cederwall, L. Timlick, S. Patterson, J. Mason, D.
520 Denton, H. Kosichek, K. Watson, and D. Dey for their contributions to the project.
521
522
523
524
525
526
527
528
529
530
531

Graphical Abstract

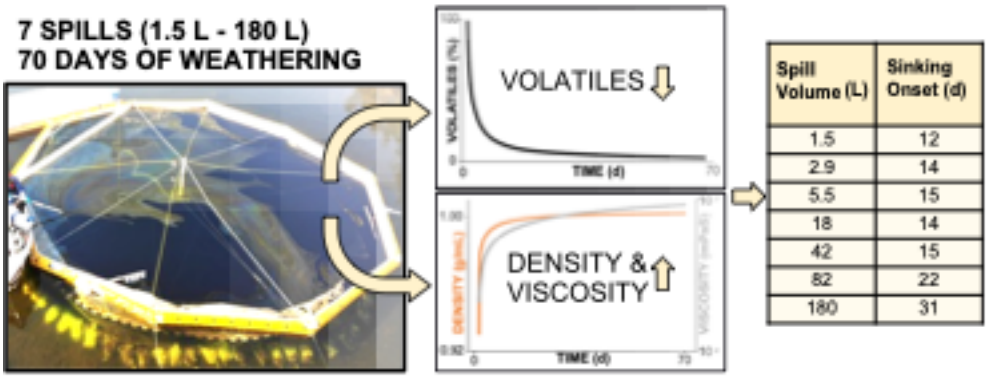

Spill Volume (L)	Sinking Onset (d)
1.5	12
2.9	14
5.5	15
18	14
42	15
82	22
180	31

Figures

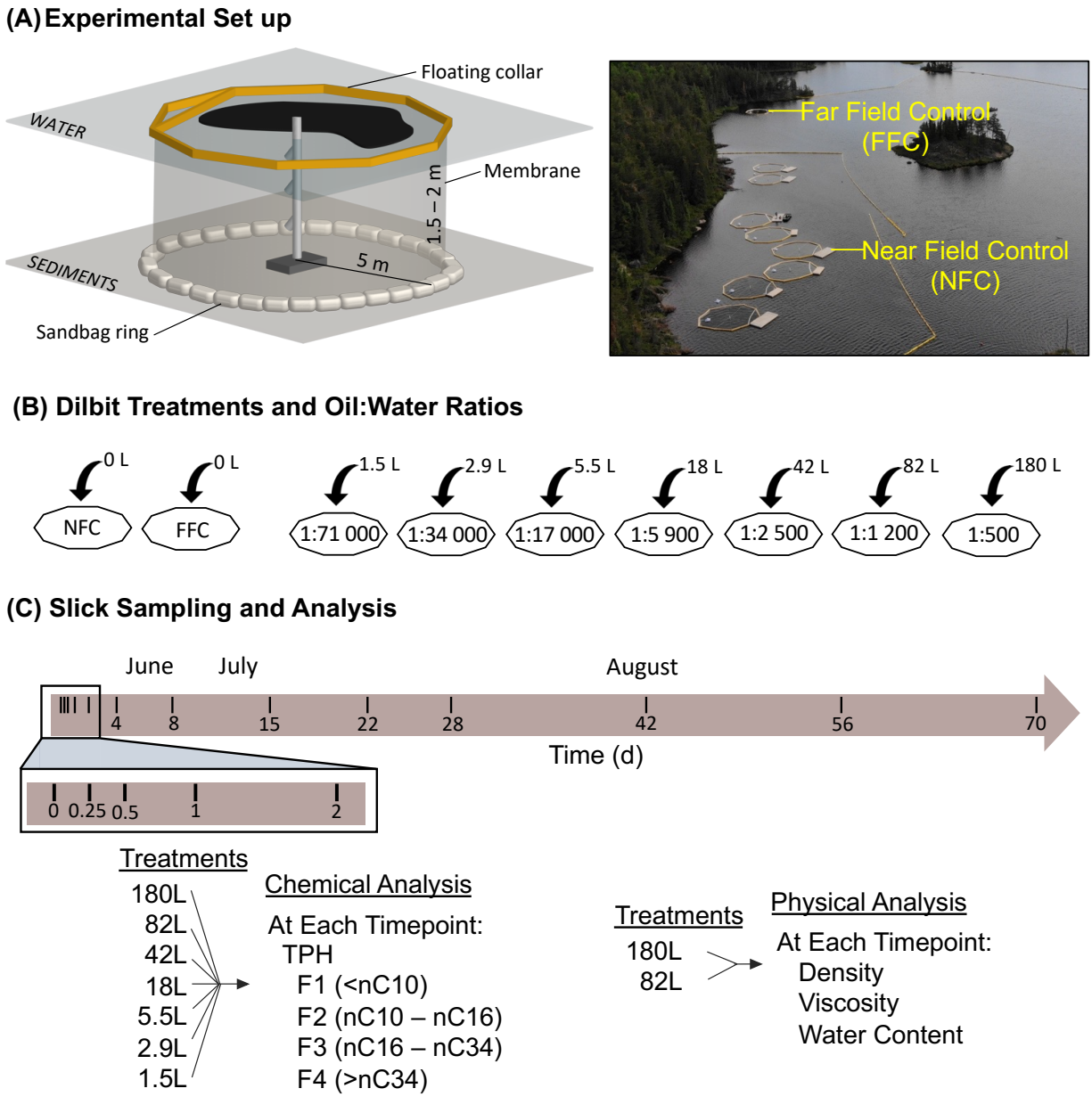

Figure 1. Experimental design of limnocorrals and simulated CLWB dilbit spills. (A) Main aspects of limnocorral and distribution of limnocorrals throughout the NW littoral zone of L260 at the IISD-ELA. (B) The distribution dilbit treatments including two controls, one near field (NFC) and one far field (FFC). (C) Overview of dilbit slick sampling timepoints and associated analyses.

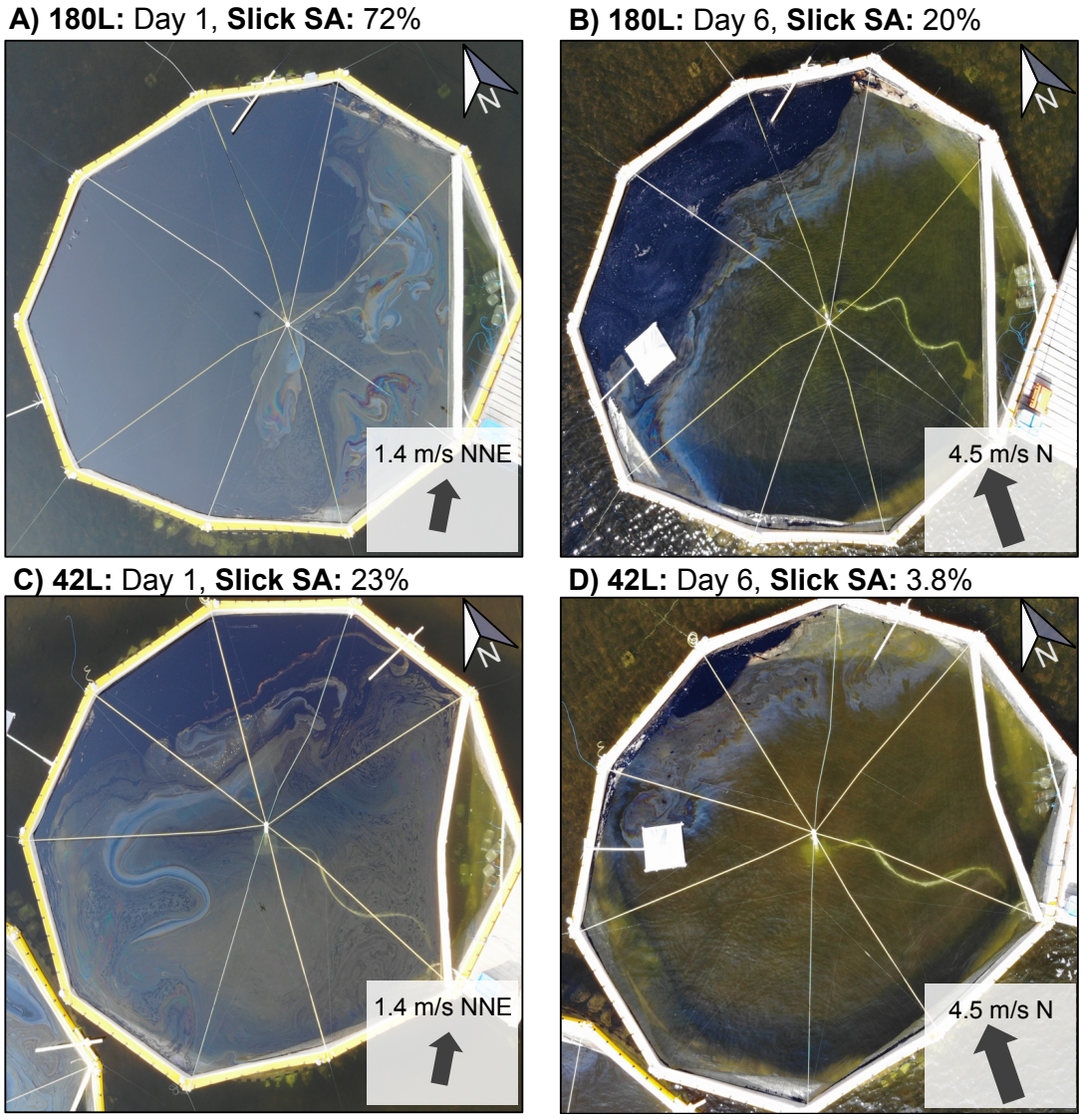

Figure 2. Aerial photographs showing changes in percentage surface area (SA) coverage of the dilbit slick from day 1 to day 6 for the 180L (A,B) and 42L treatment (C,D). North Arrows and average wind speed/direction during the time of the photo are indicated.

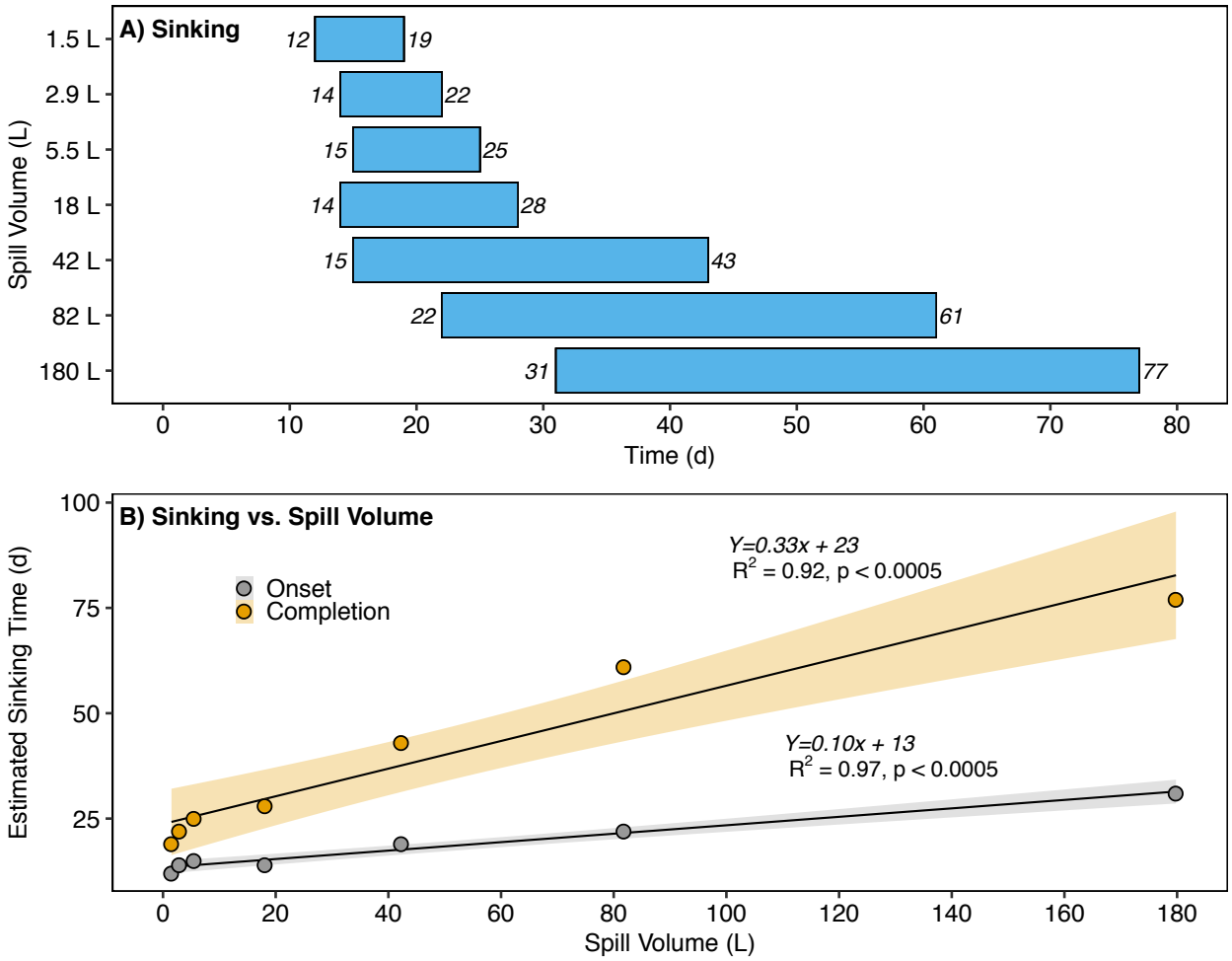

546

547 **Figure 3.** Submergence patterns observed in the seven dilbit treatments throughout the

548 experiment. The timespan between when dilbit was first noticed on the sediments and

549 when no floating dilbit slick remained (A) and the linear relationship between spill

550 volume and sinking times (B) are shown.

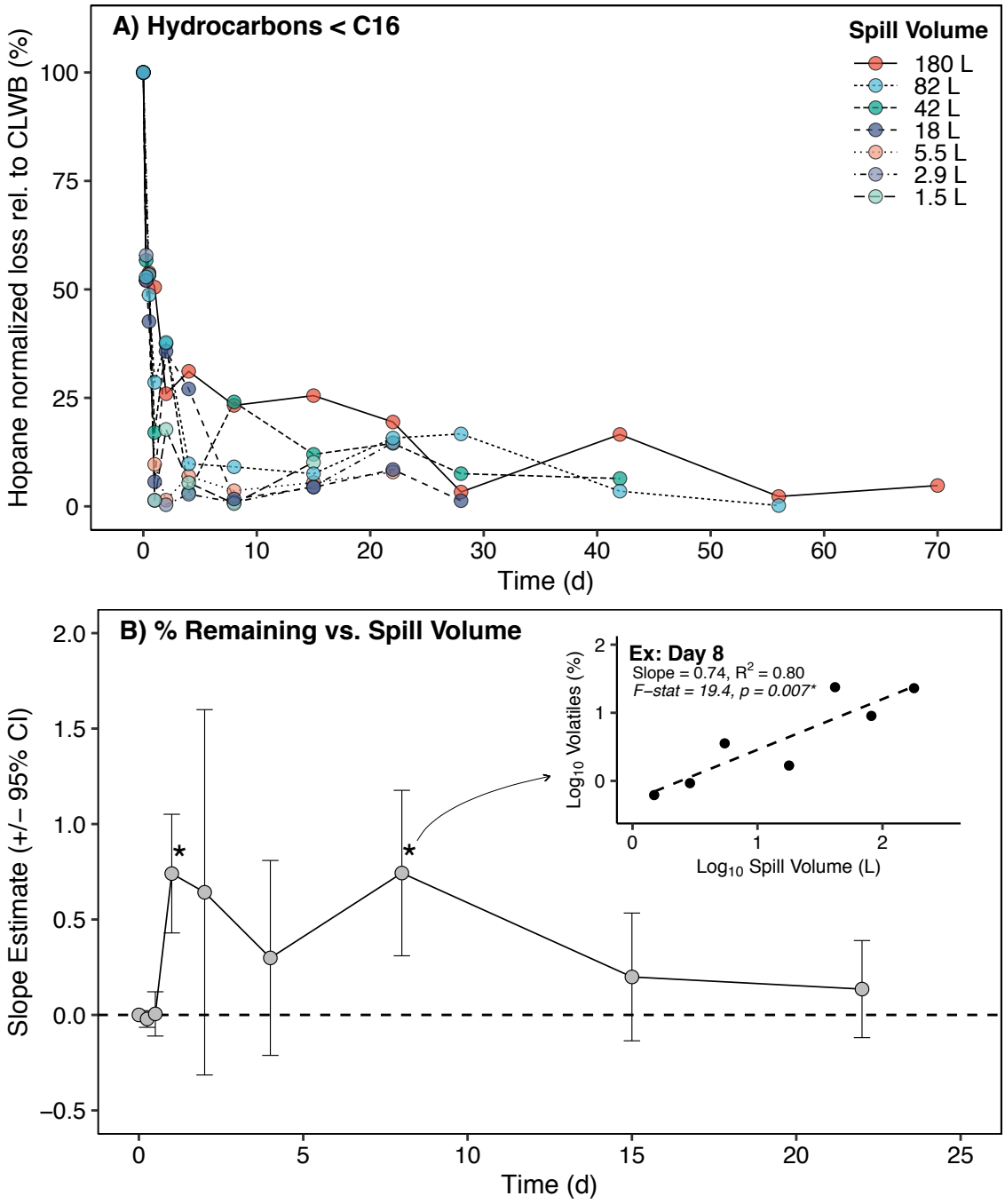

551

552 **Figure 4.** The loss of volatile hydrocarbons from surface dilbit slicks. (A) Temporal

553 changes of ≤ C_{16} hydrocarbons relative to the source dilbit in samples collected surface

554 of dilbit slicks. (B) Regression coefficients obtained by regressing hopane normalized

555 loss relative to CLWB against spill volume over time (example from day 8 shown in

556 inset). Slope estimates and 95% CI's are from individual regressions, red data points
557 are slopes significantly different from zero (i.e. $p < 0.05$). Regressions are only shown
558 up to sampling day 22 (July 12, 2018) since the majority of slicks had submerged
559 following this day yielding insufficient sample size to perform further regressions for
560 subsequent sampling days.

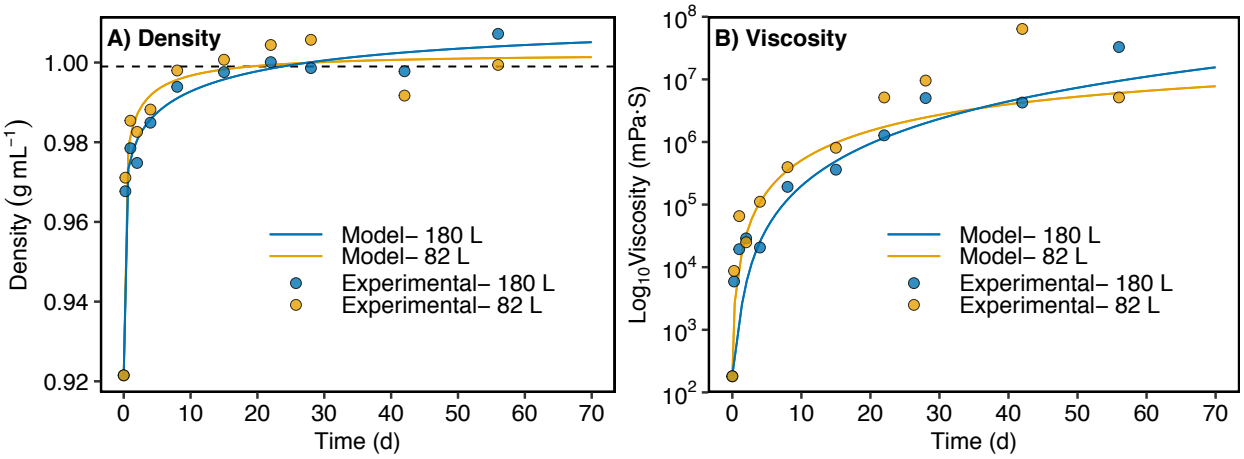

561

562 **Figure 5.** Temporal changes in (A) density (g mL^{-1}; at 15 °C) and (B) viscosity (mPa·S
563 at shear rate between 0.01 – 100 s^{-1}; at 15 °C) of samples collected from the two
564 highest treatments (82 and 180 L) throughout the experimental spills. Hyperbolic
565 models fitted to each data set are presented. The horizontal dashed line represents the
566 density of freshwater at 15 °C.

567

568

569

570

571

572

573

References

ASTM D5002-19, 2019. Standard Test Method for Density, Relative Density, and API Gravity of Crude Oils by Digital Density Analyzer. ASTM Int. West Conshohocken PA Vol 05.02. https://doi.org/10.1520/D5002-19

ASTM D7042-16, 2016. Standard test method for dynamic viscosity anddensity of liquids by Stabinger viscometer (and the calculation of kine-matic viscosity). ASTM Int. West Conshohocken PA Vol 05.04. https://doi.org/10.1520/D7042-16E03

ASTM E203-16, 2016. Standard test method for water using volumetric Karl Fischer titration. ASTM Int. West Conshohocken PA E203-16. https://doi.org/10.1520/E0203-16

Atlas, R.M., Hazen, T.C., 2011. Oil biodegradation and bioremediation: a tale of the two worst spills in US history. ACS Publications.

Baulch, H.M., Nord, T.W., Ackerman, M.Y., Dale, J.D., Hazewinkel, R.R.O., Schindler, D.W., Vinebrooke, R.D., 2003. Climate warming experiments: Design of a mesocosm heating system. Limnol. Oceanogr. Methods 1, 10–15. https://doi.org/10.4319/lom.2003.1.10

Bobra, M., Tennyson, E.J., 1989. Photooxidation of petroleum. Env. CanEnviron Prot Dir River Road 129–147.

Brandvik, P.J., Faksness, L.-G., 2009. Weathering processes in Arctic oil spills: Meso-scale experiments with different ice conditions. Cold Reg. Sci. Technol. 55, 160–166. http://dx.doi.org/10.1016/j.coldregions.2008.06.006

Canevari, G.P., 1978. Some observations on the mechanism and chemistry aspects of chemical dispersion,. ASTM Int. West Conshohocken PA Chemical dispersants for the control of oil spills, 5–17. https://doi.org/10.1520/STP35706S

CAPP, 2019. 2019 Crude Oil Forecast, Markets and Transportation (No. 2019– 0018). Canadian Association of Petroleum Producers (CAPP), Calgary, AB.

Cederwall, J., Black, T.A., Blais, J.M., Hanson, M.L., Hollebone, B.P., Palace, V.P., Rodríguez-Gil, J.L., Greer, C.W., Maynard, C., Ortmann, A.C., 2020. Life under an oil slick: response of a freshwater food web to simulated spills of diluted bitumen in field mesocosms. Can. J. Fish. Aquat. Sci. 1–10. https://doi.org/10.1139/cjfas-2019-0224

CER, 2019. Crude Oil annual Export Summary - 2018 [WWW Document]. URL www.cer-rec.gc.ca/nrg/sttstc/crdlndptrlmprdct/stt/crdlsmmr/crdlsmmr-eng.html (accessed 3.10.19).

611 CER, 2016. Canada's Energy Future 2016: Energy Supply and Demand Projections to 2040 (No.
612 ISSN 2292-1710). Canada Energy Regulator (CER).
613 Douglas, G.S., Bence, A.E., Prince, R.C., McMillen, S.J., Butler, E.L., 1996. Environmental stability
614 of selected petroleum hydrocarbon source and weathering ratios. Environ. Sci. Technol.
615 30, 2332–2339.
616 Federici, C., Mintz, J., 2014. Oil properties and their impact on spill response options literature
617 review (No. IRM-2014-U-007490). CNA Anal. Solutions, Arlington, VA, USA.
618 Fingas, M., 2015a. Review of The Properties and Behaviour of Diluted Bitumen, in: Proceeding
619 of the 39th Arctic and Marine Oil-Spill Program Technical Seminar. Environment and
620 Climate Change Canada, Vancouver, B.C., Canada, pp. 470–494.
621 Fingas, M., 2015b. Oil and Petroleum Evaporation, in: Handbook of Oil Spill Science and
622 Technology. Wiley Online Library, pp. 205–223.
623 Fingas, M., Fieldhouse, B., 2014a. Water-in-oil emulsions: formation and prediction. Handb. Oil
624 Spill Sci. Technol. 225.
625 Fingas, M., Fieldhouse, B., 2014b. Water-in-oil emulsions: formation and prediction. Handb. Oil
626 Spill Sci. Technol. 225. http://dx.doi.org/10.14355/jpsr.2014.0301.04
627 Fingas, M., Fieldhouse, B., 2004. Formation of water-in-oil emulsions and application to oil spill
628 modelling. J. Hazard. Mater. 107, 37–50.
629 http://dx.doi.org/10.1016/j.jhazmat.2003.11.008
630 Fingas, M.F., 2004. Modeling evaporation using models that are not boundary-layer regulated.
631 J. Hazard. Mater. 107, 27–36. https://doi.org/10.1016/j.jhazmat.2003.11.007
632 Fitzpatrick, F.A., Boufadel, M.C., Johnson, R., Lee, K.W., Graan, T.P., Bejarano, A.C., Zhu, Z.,
633 Waterman, D., Capone, D.M., Hayter, E., 2015. Oil-particle interactions and
634 submergence from crude oil spills in marine and freshwater environments: Review of
635 the science and future research needs (No. 2015–1076). US Geological Survey.
636 Government of Canada, Gas and Energy Research (Canada), 2014. Federal government
637 technical report - properties, composition and marine spill behaviour, fate and transport
638 of two diluted bitumen products from the Canadian oil sands.
639 Green, K.P., Jackson, T., 2015. Safety in the transportation of Oil and Gas: pipelines or rail?
640 Fraser Institute Vancouver, BC.
641 Gros, J., Nabi, D., Würz, B., Wick, L.Y., Brussaard, C.P., Huisman, J., van der Meer, J.R., Reddy,
642 C.M., Arey, J.S., 2014. First day of an oil spill on the open sea: Early mass transfers of
643 hydrocarbons to air and water. Environ. Sci. Technol. 48, 9400–9411.
644 https://doi.org/10.1021/es502437e
645 Gustitus, S.A., Clement, T.P., 2017. Formation, Fate, and Impacts of Microscopic and
646 Macroscopic Oil-Sediment Residues in Nearshore Marine Environments: A Critical
647 Review. Rev. Geophys. 55, 1130–1157. https://doi.org/10.1002/2017RG000572
648 Hansen, K., Sprague, M., Joeckel, J., Rockley, M., 2015. Response to Oil Sands Products
649 Assessment (No. CG-D-16-15). U.S, Coast Guard Research and Development Center,
650 New London, CT.
651 Harrison, W., Winnik, M.A., Kwong, P.T., Mackay, D., 1975. Crude oil spills. Disappearance of
652 aromatic and aliphatic components from small sea-surface slicks. Environ. Sci. Technol.
653 9, 231–234. https://doi.org/10.1021/es60101a006

Hollebone, B.P., Fieldhouse, B., Sergey, G., Lambert, P., Wang, Z., Yang, C., Landriault, M., 2011. The Behaviour of Heavy Oil in Fresh Water Lakes, in: Proceedings of the 34th Arctic and Marine Oilspill Program (AMOP) Technical Seminar on Environmental Contamination and Response. Environment Canada, Ottawa. pp. 668–789.

Hua, Y., Mirnaghi, F.S., Yang, Z., Hollebone, B.P., Brown, C.E., 2018. Effect of evaporative weathering and oil-sediment interactions on the fate and behavior of diluted bitumen in marine environments. Part 1. Spill-related properties, oil buoyancy, and oil-particulate aggregates characterization. Chemosphere 191, 1038–1047. https://doi.org/10.1016/j.chemosphere.2017.10.156

ITOPF, 2012. Use of Skimmers in Oil Pollution Response. International Tanker Owners Pollution Federation (ITOPF).

ITOPF, 2011. Use of dispersants to treat oil spills, Technical Information Paper 4. International Tanker Owners Pollution Federation (ITOPF), London.

Johannessen, S.C., Greer, C.W., Hannah, C.G., King, T.L., Lee, K., Pawlowicz, R., Wright, C.A., 2019. Fate of diluted bitumen spilled in the coastal waters of British Columbia, Canada. Mar. Pollut. Bull. 110691. https://doi.org/10.1016/j.marpolbul.2019.110691

Johnson, W.E., Vallentyne, J.R., 1971. Rationale, background, and development of experimental lake studies in northwestern Ontario. J. Fish. Board Can. 28, 123–128. https://doi.org/10.1139/f71-026

King, T., Toole, P., Robinson, B., Ryan, S., Lee, K., Boufadel, M.C., Li, H., Clyburne, J.A., 2019. Influence of Climatic Parameters on Changes in the Density and Viscosity of Diluted Bitumen after a Spill. J. Rnvion. Sci. Pollut. Res. 5, 373–382. https://doi.org/doi.org/10.30799/jespr.176.19050305

King, T.L., 2019. Physical properties dynamics of oil sands products and their influence on spill response (PhD Thesis). Sain Mary's University, Halifax, Nova Scotia, Canada.

King, T.L., Robinson, B., Boufadel, M., Lee, K., 2014. Flume tank studies to elucidate the fate and behavior of diluted bitumen spilled at sea. Mar. Pollut. Bull. 83, 32–37. https://doi.org/10.1016/j.marpolbul.2014.04.042

King, T.L., Robinson, B., Cui, F., Boufadel, M., Lee, K., Clyburne, J.A., 2017. An oil spill decision matrix in response to surface spills of various bitumen blends. Environ. Sci. Process. Impacts 19, 928–938. https://doi.org/10.1039/C7EM00118E

Lee, K. (chair), Boufadel, M., Chen, B., Foght, J., Hodson, P., Swanson, S., Venosa, A., 2015. Expert Panel Report on the Behaviour and Environmental Impacts of Crude Oil Released into Aqueous Environments (No. ISBN: 978-1-928140-02-3). Royal Society of Canada, Ottawa, ON, Canada.

Michel, J., Ploen, M., Elliot, J., 2014. API Study on Detection and Recovery of Sunken Oil., in: International Forum on Group V Oils. Presented at the International Spill Control Organization (ISCO), Detroit, MI.

NASEM, 2016. Spills of Diluted Bitumen from Pipelines: A Comparative Study of Environmental Fate, Effects, and Response (No. ISBN: 978-0-309-38010-2). National Academies of Sciences, Engineering and Medicine (NASEM), Washington, DC.

Nordvik, A.B., 1995. The technology windows-of-opportunity for marine oil spill response as related to oil weathering and operations. Spill Sci. Technol. Bull. 2, 17–46. https://doi.org/10.1016/1353-2561(95)00013-T

698 Oliver Wyman, 2019. Canadian Crude Oil Transportation: Comparing the Safety of Pipelines and
699 Railways, Prepared for The Railway Association of Canada. Marsh & McLennan
700 Companies.
701 Orihel, D.M., Paterson, M.J., Gilmour, C.C., Bodaly, R.A., Blanchfield, P.J., Hintelmann, H., Harris,
702 R.C., Rudd, J.W., 2006. Effect of loading rate on the fate of mercury in littoral
703 mesocosms. Environ. Sci. Technol. 40, 5992–6000. https://doi.org/10.1021/es060823+
704 Prince, R.C., Elmendorf, D.L., Lute, J.R., Hsu, C.S., Haith, C.E., Senius, J.D., Dechert, G.J., Douglas,
705 G.S., Butler, E.L., 1994. 17. alpha.(H)-21. beta.(H)-hopane as a conserved internal marker
706 for estimating the biodegradation of crude oil. Environ. Sci. Technol. 28, 142–145.
707 https://doi.org/10.1021/es00050a019
708 Prince, R.C., Garrett, R.M., Bare, R.E., Grossman, M.J., Townsend, T., Suflita, J.M., Lee, K.,
709 Owens, E.H., Sergy, G.A., Braddock, J.F., 2003. The roles of photooxidation and
710 biodegradation in long-term weathering of crude and heavy fuel oils. Spill Sci. Technol.
711 Bull. 8, 145–156. https://doi.org/10.1016/S1353-2561(03)00017-3
712 Radović, J.R., Aeppli, C., Nelson, R.K., Jimenez, N., Reddy, C.M., Bayona, J.M., Albaigés, J., 2014.
713 Assessment of photochemical processes in marine oil spill fingerprinting. Mar. Pollut.
714 Bull. 79, 268–277. https://doi.org/10.1016/j.marpolbul.2013.11.029
715 Rodriguez-Gil, J.L., Stoyanovich, S., Hanson, M., Hollebone, B., Palace, V., Orihel, D., Black, T.,
716 Cederwall, J., Mason, J., Patterson, S., Timlick, L., Séguin, J., Blais, J., In Prep. Simulating
717 diluted bitumen spills in boreal lake limnocorrals - Part 1: system description and water
718 column concentrations of hydrocarbons and metals.
719 Short, J.W., 2013. Susceptibility of Diluted Bitumen Products from the Alberta Tar Sands to
720 Sinking in Water (No. D72-80–2). JWS Consulting LLC.
721 Stout, S.A., Wang, Z., 2016. Chemical fingerprinting methods and factors affecting petroleum
722 fingerprints in the environment. Stand. Handb. Oil Spill Environ. Forensics 61–129.
723 Stoyanovich, S., Yang, Z., Hanson, M., Hollebone, B., Orihel, D., Palace, V., Rodriguez-Gil, J.,
724 Faragher, R., Mirnaghi, F., Shah, K., Blais, J., 2019. Simulating a spill of diluted bitumen:
725 Environmental weathering and submergence in a model freshwater system. ET&C.
726 https://doi.org/10.1002/etc.4600
727 Transport Canada, 2014. A Review of Canada's Ship-Source Spill Preparedness and Response:
728 Setting the Course for the Future, Phase II, Requirements for the Arctic and for
729 Hazardous and Noxious Substances Nationally (No. ISBN 978-1-100-24991-9). Tanker
730 Safety Panel Secretariat Ottawa, Canada.
731 Transport Canada, 2013. Tanker Safety Expert Panel - A review of Canada's Ship-source Oil Spill
732 Preparedness And Response Regime: Setting the course for the future (No. ISBN 978-1-
733 100-54627-8). Tanker Safety Panel Secretariat Ottawa, Canada.
734 Transport Canada, 1995. Response Organization Standards. Marine Safety Directorate, Ottawa,
735 Canada.
736 Transportation Research Board and National Research Council, 2014. TRB Special Report 311:
737 Effects of Diluted Bitumen on Crude Oil Transmission Pipelines (No.
738 https://doi.org/10.17226/18381). The National Academies Press, Washington, DC.
739 US EPA, 2013. Dredging Begins on Kalamazoo River, Enbridge Oil Spill, Marshall, Michigan. U.S.
740 Environmental Protection Agency (US EPA).

741 Venosa, A.D., Suidan, M.T., King, D., Wrenn, B.A., 1997. Use of hopane as a conservative
742 biomarker for monitoring the bioremediation effectiveness of crude oil contaminating a
743 sandy beach. J. Ind. Microbiol. Biotechnol. 18, 131–139.
744 https://doi.org/10.1038/sj.jim.2900304
745 Wadsworth, T., 1995. Containment & Recovery of Oil Spills at Sea: Methods and Limitations.
746 Warnock, A.M., Hagen, S.C., Passeri, D.L., 2015. Marine tar residues: a review. Water. Air. Soil
747 Pollut. 226, 68. https://doi.org/10.1007/s11270-015-2298-5
748 Waterman, D.M., Garcia, M.H., 2015. Laboratory Tests of Oil-Particle Interactions in a
749 Freshwater Riverine Environment with Cold Lake Blend Weathered Bitumen. Ven Te
750 Chow Hydrosystems Lab. Univ. Ill.
751 Weast, R.C., Astle, M.J., Beyer, W.H., 1988. CRC handbook of chemistry and physics. CRC press
752 Boca Raton, FL.
753 Yang, C., Lambert, P., Zhang, G., Yang, Z., Landriault, M., Hollebone, B., Fieldhouse, B., Mirnaghi,
754 F., Brown, C.E., 2017. Characterization of chemical fingerprints of unconventional
755 Bakken crude oil. Environ. Pollut. 230, 609–620.
756 https://doi.org/0.1016/j.envpol.2017.07.011
757 Yang, Z., Hua, Y., Mirnaghi, F., Hollebone, B.P., Jackman, P., Brown, C.E., Yang, C., Shah, K.,
758 Landriault, M., Chan, B., 2018. Effect of evaporative weathering and oil-sediment
759 interaction on the fate and behavior of diluted bitumen in marine environments. Part 2.
760 The water accommodated and particle-laden hydrocarbon species and toxicity of the
761 aqueous phase. Chemosphere 191, 145–155.
762 https://doi.org/10.1016/j.chemosphere.2017.10.033
763 Yarranton, H., Motahhari, H.R., Schoeggl, F., Zhou, J.Z., 2015. Evaporative Weathering of Diluted
764 Bitumen Films. J. Can. Pet. Technol. 54, 223–244. https://doi.org/10.2118/174557-PA
765 Zhao, L., Torlapati, J., Boufadel, M.C., King, T., Robinson, B., Lee, K., 2014. VDROP: A
766 comprehensive model for droplet formation of oils and gases in liquids-Incorporation of
767 the interfacial tension and droplet viscosity. Chem. Eng. J. 253, 93–106.
768 https://doi.org/10.1016/j.cej.2014.04.082
769